JOURNAL OF VIROLOGY, Dec. 1997, p. 8955–8961 Vol. 71, No. 12
0022-538X/97/$04.00+0

Hexon-Only Binding of VP26 Reflects Differences between the Hexon and Penton Conformations of VP5, the Major Capsid Protein of Herpes Simplex Virus

PAUL T. WINGFIELD,[1] STEPHEN J. STAHL,[1] DARRELL R. THOMSEN,[2] FRED L. HOMA,[2] FRANK P. BOOY,[3] BENES L. TRUS,[3,4] AND ALASDAIR C. STEVEN[3]*

Protein Expression Laboratory[1] and Laboratory of Structural Biology,[3] National Institute of Arthritis and Musculoskeletal and Skin Diseases, and Computational Bioscience and Engineering Laboratory, Division of Computer Research and Technology,[4] National Institutes of Health, Bethesda, Maryland 20892, and Pharmacia & Upjohn Inc., Kalamazoo, Michigan 49007[2]

Received 12 June 1997/Accepted 26 August 1997

VP26 is a 12-kDa capsid protein of herpes simplex virus 1. Although VP26 is dispensable for assembly, the native capsid (a T=16 icosahedron) contains 900 copies: six on each of the 150 hexons of VP5 (149 kDa) but none on the 12 VP5 pentons at its vertices. We have investigated this interaction by expressing VP26 in *Escherichia coli* and studying the properties of the purified protein in solution and its binding to capsids. Circular dichroism spectroscopy reveals that the conformation of purified VP26 consists mainly of β-sheets (~80%), with a small α-helical component (~15%). Its state of association was determined by analytical ultracentrifugation to be a reversible monomer-dimer equilibrium, with a dissociation constant of $\sim 2 \times 10^{-5}$ M. Bacterially expressed VP26 binds to capsids in the normal amount, as determined by quantitative sodium dodecyl sulfate-polyacrylamide gel electrophoresis. Cryoelectron microscopy shows that the protein occupies its usual sites on hexons but does not bind to pentons, even when available in 100-fold molar excess. Quasi-equivalence requires that penton VP5 must differ in conformation from hexon VP5: our data show that in mature capsids, this difference is sufficiently pronounced to abrogate its ability to bind VP26.

The capsid of herpes simplex virus type 1 (HSV-1) is an exceptionally large and elaborate viral particle. Approximately 1,250 Å in diameter, the shell of the mature capsid is made up of ~3,000 protein molecules, with a total mass of ~200 MDa (reviewed in references 28 and 34). In addition to a still indeterminate number of minor components, the shell contains four abundant proteins; 960 copies of VP5 (149 kDa), the major capsid protein, form the 150 hexons and 12 pentons that pack together in the icosahedral surface lattice. At the 320 sites of threefold symmetry are triplexes, which are heterotrimers—probably with an $\alpha_2\beta$ stoichiometry (24)— of VP23 (35 kDa) and VP19c (50 kDa). These three proteins are all essential for capsid assembly, as is an internal scaffolding protein, pre-VP22a (35 kDa), of which >1,000 copies coassemble with the shell proteins to form the procapsid (23, 37). This precursor capsoid subsequently undergoes a structural transformation to yield the mature shell. In vivo maturation involves proteolytic processing of pre-VP22a to VP22a and its expulsion from the capsid.

In addition to the three essential shell proteins—VP5, VP19c, and VP23—the HSV-1 capsid contains a fourth abundant protein (8, 17), now called VP26, of relatively low molecular mass (12 kDa). Although VP26 is dispensable for assembly (35, 36), it is incorporated into the capsid in large amounts, approximately equimolar with VP5 (24). The sites that VP26 occupies have been determined by cryo-electron microscopy, based on difference imaging. A comparison between pentonless capsids with and without VP26 localized this protein to the tips of hexons (7). From subtracting one-fifth of a penton from one-sixth of a hexon from the same density map of intact capsids, Zhou et al. concluded that VP26 is absent from pentons (43). This proposal—which assumes that any structural differences between the hexon and penton states of VP5 are relatively slight—was corroborated by direct comparison between intact capsids with and without VP26 (38, 42). Thus, the copy number of VP26 should be 900, if one assumes 100% occupancy of the hexon binding sites.

While there is now consensus as to the location of VP26, the nature of the molecular mechanism that excludes it from pentons has been less clear. We have proposed that it is a consequence of conformational differences between hexon VP5 and penton VP5 (38). Such differences are manifested in other ways, including dissimilar binding reactivities to hexons and pentons of three monoclonal antibodies (39), differential sensitivity to proteolysis (33), and differential susceptibility to extraction from the capsid (7, 22). Alternatively, Zhou et al. (42) have proposed a symmetry-mismatch mechanism, whereby VP26 is envisaged to form hexamers in solution that fit on to VP5 hexons but not on to pentons.

To investigate the properties of VP26 in greater depth, we have expressed its gene—UL35 (13, 21)—in *Escherichia coli*, purified the protein, and studied its properties, including its propensity to oligomerize and to bind to capsids.

MATERIALS AND METHODS

Protein expression in *E. coli*. HSV VP26 was produced as a C-terminal fusion protein with glutathione *S*-transferase (GST), using vector pGEX-4T-3 (Pharmacia Biotech, Piscataway, N.J.). The DNA fragment encoding VP26 was generated from pAcUL35 (36), using PCR as previously described (31), and cloned into the *Bam*HI site of pGEX-4T-3. The resulting plasmid, pGEX-HSV-VP26, encodes the first 220 amino acids of GST, 6 amino acids containing the thrombin cleavage site (Leu-Val-Pro-Arg-†-Gly-Ser, with † indicating the cleavage site), followed by His and the 112 amino acids of VP26. Thrombin cleavage of the fusion protein should release the VP26 moiety with an additional Gly-Ser-His at the N terminus. *E. coli* RB 791 was transformed with the expression plasmid and

* Corresponding author. Mailing address: Bldg. 6, Room B2-34, 6 Center Dr., MSC 2717, National Institutes of Health, Bethesda, MD 20892-2717. Phone: (301) 496-0132. Fax: (301) 480-7629. E-mail: Alasdair_Steven@NIH.GOV.

grown in 2× LB (pH 7) at 37°C and 30% pO_2 in a 2-liter model MD fermentor (Braun Biotech, Melsungen, Germany). Protein expression was induced with 2 mM isopropylthiogalactoside (IPTG) at 37°C for 4 h.

Purification of the fusion protein. Pelleted cells (50 g) were resuspended in 100 ml of 100 mM Tris-HCl (pH 7.5) containing 5 mM dithiothreitol (DTT) and 5 mM EDTA (break buffer), lysed by passage through a French pressure cell at 16,000 lb/in^2, and then sonicated at full power, 50% duty cycle, on ice for 5 min. The lysate was centrifuged in a JA-14 rotor (Beckman Instruments, Palo Alto, Calif.) at 13,000 rpm (26,000 × *g*) at 4°C for 45 min. The pellet was washed once by resuspension in 200 ml of break buffer containing 1% Triton X-100 and centrifugation at 26,000 × *g* and then washed a second time with break buffer alone. The pellet from the second wash was resuspended in 50 ml of 50 mM Tris-HCl containing 8 M guanidine-HCl (Gdn-HCl) and 10 mM DTT and then centrifuged in a Ti45 rotor at 35,000 rpm (95,000 × *g*) for 30 min at 4°C. The clear supernatant (50 ml) was applied to a Superdex 200 column (6 cm [diameter] by 60 cm [length]) equilibrated with 50 mM Tris-HCl containing 4 M Gdn-HCl and 5 mM DTT (S200 buffer). The column was loaded and eluted at 5 ml/min. Fractions were assayed for GST-VP26 by sodium dodecyl sulfate-polyacrylamide gel electrophoresis (SDS-PAGE) on 4 to 20% gels (Novex, San Diego, Calif.) following precipitation with 90% ethanol (26). The pooled fusion protein was stored at −80°C until required.

Digestion of the fusion protein and refolding of VP26. GST-VP26 in S200 buffer was diluted to about 0.75 to 1.0 mg/ml with the same buffer and then dialyzed, first against 50 mM Tris-HCl (pH 8.0) containing 0.15 M NaCl, 2.5 M urea, 10 mM 3-[(3-cholamidopropyl)-dimethylammonio]-1-propanesulfonate (CHAPS; Calbiochem, La Jolla, Calif.), and 2 mM EDTA and then against the same buffer minus the urea. The slightly cloudy solution was clarified by centrifugation at 5,000 × *g* for 20 min. Thrombin (catalog no. T6884; Sigma Chemical, St. Louis, Mo.) was then added to the supernatant to a concentration of 0.5% (wt/wt; an $A_{0.1\%}$ of 1.8 at 280 nm was used to estimate the protease concentration). The solution was incubated for 1.5 h at ~22°C, the same amount of thrombin was added, and the digestion continued for a further 1.5 h, whereupon it was quenched by adding 0.1 mM phenylmethylsulfonate fluoride from a 0.1 M stock in dry ethanol. Solid Gdn-HCl was added to 8 M, and the solution was applied to a column of Superdex 200 equilibrated in S200 buffer. VP26-containing fractions were identified by SDS-PAGE, performed as described above. To the pooled fractions, 10 mM CHAPS was added, and the solution was dialyzed, first against 50 mM Tris-HCl (pH 7.5) containing 2.5 M urea, 10 mM CHAPS, and 0.25 M NaCl and then against same buffer minus the urea. As VP26 does not contain any cysteine residues, reductant was not included in the final folding buffer or in any of the buffers used in the studies described below. The folded protein was concentrated in a Centriprep-10 centrifugal ultrafiltration device (Amicon-Millipore, Bedford, Mass.) and sterile filtered through Millex-GV 0.22-μm-pore-size filters (Millipore).

The concentrations of purified GST-VP26 and VP26 were determined by measuring the absorbancies at 280 nm in a 1-cm-path-length cell, using a double-beam, diode array, UV/VIS spectrophotometer (model 8450A; Hewlett-Packard, Palo Alto, Calif.). Molar absorbance coefficients were calculated from the amino acid compositions according to Wetlaufer (41), yielding values of 48.3 $mM^{-1} \cdot cm^{-1}$ ($A_{0.1\%}$ = 1.25) and 7.02 $mM^{-1} \cdot cm^{-1}$ ($A_{0.1\%}$ = 0.57) for GST-VP26 and VP26, respectively.

Protein sequencing and mass spectrometry. Samples in solution were applied to polyvinylidene difluoride membranes by using a ProSpin preparation cartridge (Perkin-Elmer, Foster City, Calif.). Proteins resolved by SDS-PAGE were electroblotted onto ProBlott membranes as instructed by the manufacturer (Perkin-Elmer). Automated Edman degradation was performed by using a Blott cartridge (Perkin-Elmer) and an Applied Biosystems model 477A protein sequencer. The molecular weight of VP26 was measured with a model G203AQ matrix-assisted laser desorption time-of-flight (MALDI-TOF) mass spectrometer (Hewlett Packard).

Circular dichroism. Spectra were recorded at 22°C on a J-720 spectropolarimeter (Jasco Inc., Easton, Md.). Measurements in the far UV (180 to 260 nm) were made by using either 0.01- or 0.02-cm-path-length cells and a 1-nm bandwidth. The protein concentration was 0.5 to 1.0 mg/ml. The protein buffer was exchanged for 50 mM sodium phosphate (pH 7.2)–250 mM NaCl, plus or minus 10 mM CHAPS, using a PD-10 column (Pharmacia Biotech). Immediately prior to use, solutions were filtered with Millex-GV 0.22-μm-pore-size filter units and degassed. Secondary structure was estimated from the spectra by the CONTIN method (27).

Analytical ultracentrifugation. A Beckman Optima XL-A analytical ultracentrifuge with an An-60Ti rotor and standard double-sector centerpiece cells was used. Centrifugation at 23,000 rpm was for 14 to 20 h at 20°C. The protein buffer used in most experiments was 50 mM Tris-HCl (pH 7.5)–0.25 M NaCl–10 mM CHAPS, but analyses were also performed with the NaCl concentration increased to 0.5 M or with the CHAPS concentration reduced to 5 or 0 mM. Baseline corrections were established by overspeeding at 45,000 rpm for 4 h. Data were analyzed with the Beckman Origin software. The partial specific volume of VP26 was calculated from its amino acid composition (9) to be 0.724 ml/g at 10°C (0.720 at 20°C). The solvent density was calculated as described previously (18). To calculate the dissociation constant for VP26, a monomer mass of 12,377 and the extinction coefficient given above were used.

Capsid production. Capsids were assembled by infecting Sf9 cells with recombinant baculoviruses expressing HSV capsid genes and purified as previously described (36, 38). Briefly, combinations of baculoviruses expressing all six HSV-1 capsid genes (ALL) or expressing all except the UL35 gene [(ALL − UL35)] were expressed in Sf9 insect cells. At 64 h postinfection, cells were harvested, and ALL and (ALL − UL35) capsids were purified (separately) by two cycles of sucrose gradient centrifugation.

Binding of VP26 to HSV-1 capsids. Purified (All − UL35) capsids at ~1 mg/ml in phosphate-buffered saline (PBS) were mixed with various amounts of VP26 (see Results) in a final reaction volume of 100 μl and incubated for 30 min at 22°C. Immediately beforehand, the VP26 was centrifuged at 100,000 × *g* for 30 min, and the supernatant was taken for use in the binding reaction. After the incubation, the capsids were pelleted by centrifugation at 20,000 × *g* for 30 min at 4°C, washed twice by resuspension in 200 μl of PBS and repelleting, and finally resuspended in 50 μl of PBS. Binding reactions were also carried out in the presence of 7.5 mM CHAPS. Samples were run on 4 to 20% polyacrylamide gels (Novex) according to the manufacturer's instructions. Protein bands stained with Coomassie blue were quantitated by using a PDI 325oe optical scanner and software (PDI, New York, N.Y.).

Cryo-electron microscopy. Grids bearing vitrified capsid-containing films were prepared from 5-μl drops of suspensions of capsids at 2 to 3 mg of protein per ml in PBS as described by Booy et al. (5). These specimens were observed in a Philips EM400RT electron microscope equipped with a liquid-N_2-cooled Gatan 626 cryo-holder and modified anticontamination blades, using minimal-dose procedures at a magnification of ×36,000.

Three-dimensional image reconstruction. For digital analysis, we selected three micrographs which had suitably dense distributions of particles (e.g., Fig. 5a) and, as determined by optical diffraction, no significant astigmatism or drift. Their defocus values were such that the first zero of the contrast transfer function lay at frequencies of about (29.0 Å)$^{-1}$, (25.2 Å)$^{-1}$, and (29.0 Å)$^{-1}$, respectively. These images were scanned at 6.6 Å per pixel on a Perkin-Elmer PDS-1010MG microdensitometer. Since all three micrographs were recorded in the same series, they were assumed to have the same magnification. Individual capsid images were extracted by means of the X3DPREPROCESS program (10). Their orientations were solved and refined by using the Polar Fourier Transform program (1), taking an earlier reconstruction (11) as the starting model. The 159 particles with the highest correlation coefficients (out of a total of 282) were used to calculate a density map to a resolution limit of 24 Å, by Fourier-Bessel synthesis (2, 3, 12, 15). The phases of the terms beyond the first contrast transfer function zero were inverted in the individual Fourier transforms prior to calculating the reconstruction.

RESULTS

Expression and purification of VP26. Initially, we attempted to express VP26 directly in *E. coli* but were unsuccessful. However, expression as a GST fusion resulted in substantial synthesis (5 to 10% of cell protein) of a protein in the expected molecular mass range, i.e., ~38 kDa. This protein was insoluble and consequently was extracted in Gdn-HCl and then fractionated to about 75% purity by gel filtration, also in Gdn-HCl (Fig. 1, lane 2). Previous work had shown that VP26 extracted from capsids with Gdn-HCl could be rebound to capsids—and, by inference, refolded—upon removal of the denaturant (7, 22).

VP26 was detached from the 26-kDa GST by thrombin digestion. Prior to digestion, the fusion protein was folded by equilibrium dialysis, using a buffer containing the zwitterionic detergent CHAPS (10 mM) and 0.15 M NaCl. In this buffer, a compromise was achieved between maintaining the solubility of the substrate and products (with CHAPS and salt) and activity of the thrombin (inhibited by high salt concentrations). VP26 was separated from the GST moiety and thrombin and further purified by gel filtration under denaturing conditions (Fig. 1). Purified VP26 was adjusted to ~0.5 mg/ml in 8 M Gdn-HCl and refolded by using buffers containing 10 mM CHAPS and moderately high ionic strength (0.25 to 0.5 M NaCl). Both components appeared necessary to prevent gradual aggregation. The purity of the resulting material is demonstrated by SDS-PAGE in Fig. 1 (lane VP26). The only detectable contaminants are trace amounts of breakdown products of slightly lower molecular weight (MW) (see the legend to Fig. 1).

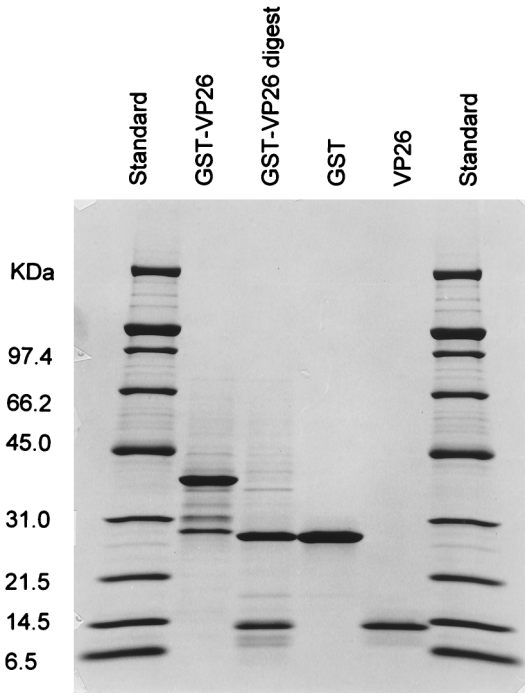

FIG. 1. Expression of HSV-1 VP26 in *E. coli* as a GST fusion protein and its subsequent purification, as monitored by SDS-PAGE. Starting with ~50 g (wet weight) of cells, about 850 mg of the GST-fusion protein (lane 2) was recovered, using a two-stage dialysis scheme (see Materials and Methods). Following thrombin digestion, which was essentially complete (cf. lane 3), gel filtration followed by the second refolding yielded a 60 to 70% recovery of purified VP26 (lane 5), separated from GST (lane 4); 1.5 to 2.0 mg of VP26 was obtained per g (wet weight) of cells. Trace amounts of two contaminants of slightly lower MWs remain. They appear to arise from thrombin side reactions which generate small amounts of both N- and C-terminally truncated VP26 and a N-terminal fragment of the mature GST protein (data not shown). Interestingly, small amounts of lower-MW forms were also observed in VP26 extracted from native capsids (5), although in this case, they may represent phosphorylated forms (20).

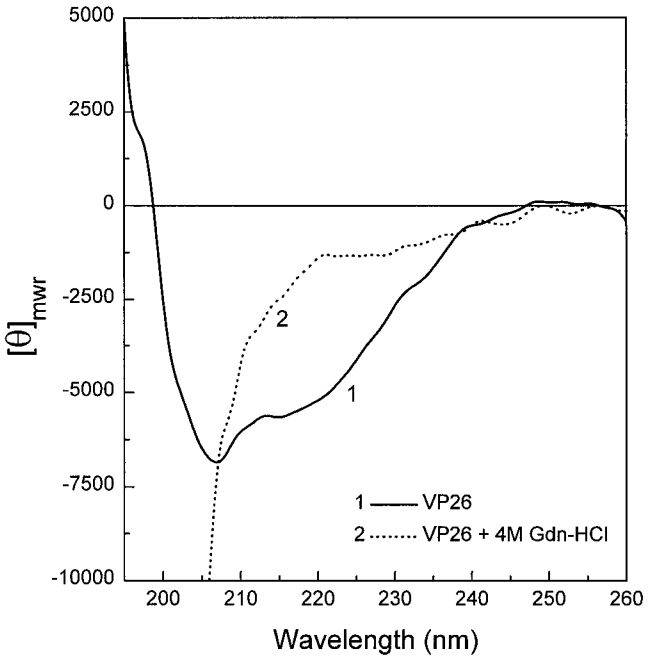

FIG. 2. Circular dichroic spectrum of HSV-1 VP26 (spectrum 1). Protein incubated with Gdn-HCl (spectrum 2) evinces a loss of ellipticity at 220 nm and a large increase at 206 to 204 nm, typical of denatured proteins (40), thus emphasizing that the VP26 was originally folded. The spectra are shown in far-UV region to limits of reliable detection as monitored by photomultiplier voltage (usually less than 600 V). The units of the ordinates are mean residue ellipticity $[\theta]_{mwr}$ and have the dimensions deg · cm^2 · $dmol^{-1}$.

Identification of the expressed protein. To confirm that the protein isolated was VP26, its N-terminal amino acid sequence was determined. The first five residues were Gly-Ser-His-Met-Ala, indicating that processing had occurred as expected, between Arg and Gly of the thrombin cleavage site (see Materials and Methods). The protein's identity as VP26, extended by three residues at its amino terminus, was further established by MALDI-TOF mass spectrometry, which yielded a mass value within 0.05% of that predicted from the DNA coding sequence (i.e., 12,377).

Secondary structure. The overall conformation of VP26 was examined by far-UV circular dichroism (Fig. 2, spectrum 1). A similar spectrum was obtained when CHAPS was omitted from the buffer, indicating that the detergent has no apparent effect on the overall structure of VP26. Comparison with the random coil obtained after denaturation with Gdn-HCl (Fig. 2, spectrum 2) indicates that, as purified, VP26 has a well-defined secondary structure and is therefore likely to be partly if not completely folded. From these data, its secondary structure was estimated to be mainly β-sheet (~80%), with some α-helical contribution (13 to 15%). These values concur with those predicted (75% β-strand plus turn; 25% α-helix) by the neural network-based PHD program (30). In the aromatic region, i.e., 340 to 260 nm, its spectrum (not shown) is weak, most likely due to the single Trp and Tyr residues being located in flexible regions.

Oligomeric status of VP26. The MW of VP26 was determined by sedimentation equilibrium. During the centrifugation runs (14 to 16 h at 10 to 20°C), the protein was equally well behaved in 5 to 10 mM CHAPS with 0.25 to 0.5 M NaCl. At equilibrium, the protein concentration gradient increased from 0.01 mg/ml at the top to approximately 2.5 mg/ml at the bottom of the cell, depending on the concentration of the starting sample. Conversion of these data to plots of MW versus concentration (not shown) indicated that the MW increased as a function of radial position. The overall weight-average MW was 18,000 to 20,000, intermediate between those of a monomer (12,377) and a dimer (24,754). Extrapolating to the highest concentrations (bottom of cell) gave MWs approaching that of the dimer. These findings suggest that in the buffer used, VP26 is a reversible monomer-dimer system. A good fit to the data was obtained, using this model with a dissociation constant of 2×10^{-5} M (Fig. 3). It follows that VP26 was 40 to 60% monomeric at the concentrations used in the binding studies described below, i.e., 4 to 16 μM.

When the same data were fitted for alternative models such as monomer-trimer, monomer-tetramer, monomer-pentamer, or monomer-hexamer equilibria, or an ideal (noninteracting) mixture of monomers and hexamers, poor agreement was obtained, with higher residuals and systematic trends in their residual plots (data not shown). In contrast, the residuals from the monomer-dimer model scatter randomly about the zero value (Fig. 3), which is a hallmark of a good fit. In particular, the chi-square statistic for the monomer-hexamer model was almost 20-fold higher than that for the successful monomer-dimer model.

Binding of purified VP26 to HSV-1 capsids. To test our bacterially expressed VP26 for competence to bind to capsids, the purified protein was mixed with (All − UL35) capsids (35)

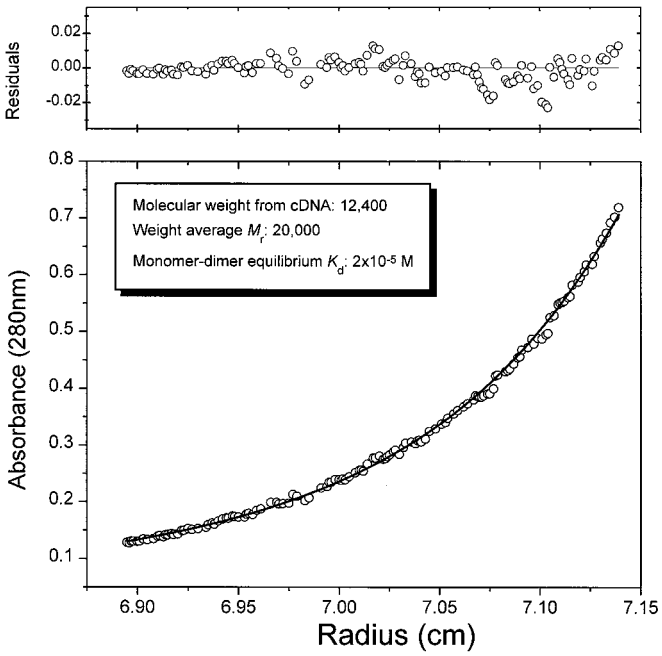

FIG. 3. Sedimentation equilibrium analysis of HSV-1 VP26. Measurements were made by using a Beckman Optima XL-A analytical ultracentrifuge, running at 23,000 rpm. The absorbance gradient in the centrifuge cell after attaining sedimentation equilibrium is shown in the bottom panel. The solid line is the result of the fit using reversible monomer-dimer model, and the open circles are the experimental values. The top panel shows the differences between the fitted and experimental values as a function of radial position (residuals).

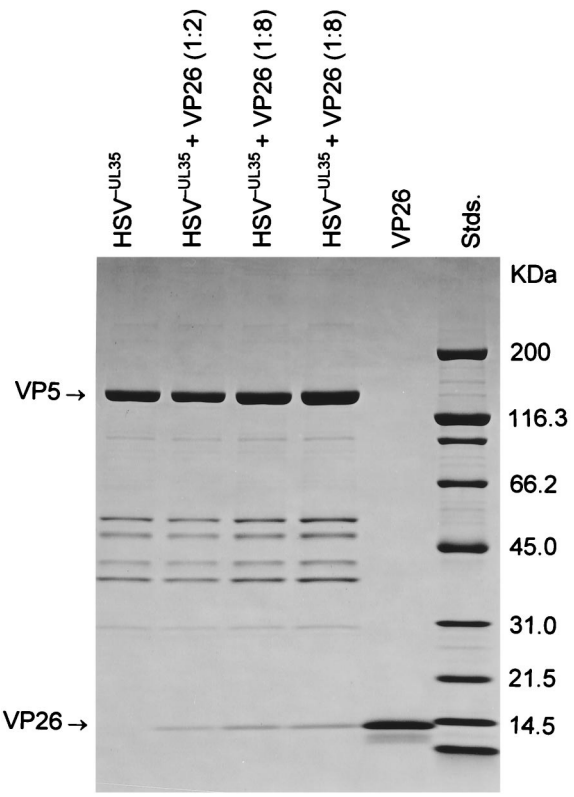

FIG. 4. Binding of purified VP26 to HSV-1 capsids, as monitored by SDS-PAGE on a 4 to 20% gradient gel stained with Coomassie blue. These (All − UL35) capsids (denoted here as HSV^{-UL35}) lack VP26 (lane 1). After complementation with twofold (lane 2) and eightfold (duplicates in lanes 3 and 4) molar excesses of VP26, the capsids were separated from unreacted VP26 by two wash cycles. The amount of VP26 retained was essentially the same in all three samples and in the same proportion relative to the major capsid protein, VP5, as in wild-type capsids (24). The purified VP26 is shown in lane 5. Stds., size standards.

(Fig. 4). The molar ratios of VP26 to VP5 were 2:1 and 8:1, respectively, in two parallel incubations. Unbound VP26 was removed by two cycles of pelleting the capsids, discarding the supernatants, and resuspending the pellets in buffer. Analysis of the washed capsids by SDS-PAGE (Fig. 4) clearly indicated binding of VP26. The molar ratios of VP5 to VP26 were determined by densitometric analysis to be ~1:1.16 for the twofold incubation and 1:1.24 for the eightfold incubation. We conclude that in both cases, VP26 bound to the capsids in saturating amounts, close to the theoretical value for wild-type capsids (i.e., 1:0.95 [see the introduction]). When these experiments were repeated in CHAPS-containing buffer similar to that used for analytical ultracentrifugation, essentially identical binding of VP26 to capsids was observed (data not shown).

Visualization of bound VP26. To determine the sites on the capsid surface to which VP26 had bound, a sample of capsids from the incubation at eightfold molar excess was examined by cryo-electron microscopy (Fig. 5a) and three-dimensional image reconstruction. The outer surface of the resulting density map is shown in Fig. 5b. The six "horns" of density around the rim of each hexon, associated with six VP26 monomers, are clearly present, whereas these features are absent from pentons. This conclusion was confirmed by inspecting sections through the map, which show all levels of density coded as gray levels (data not shown). These images contained no density above background in the regions overlying the penton tips, implying no detectable level of occupancy by VP26.

In principle, the absence of VP26 from the pentons of native capsids might reflect a limited supply of VP26 in the nuclei of infected cells, combined with a preference for hexons over pentons, rather than complete inability of VP26 to bind to pentons. That the latter proposition is correct is attested by this experiment, in which, after saturation of the hexon sites, the remaining VP26 did not bind to pentons despite being available in high excess, i.e., at a molar ratio of ~100:1 relative to penton VP5.

DISCUSSION

Now that the molecular anatomy of the herpesvirus capsid has been defined—at least for its major constituents (34)—attention is shifting to the interactions that control assembly and maturation. These include the interactions responsible for the import of capsid proteins from the cytoplasm to the nucleus, the interactions whereby subunits associate into assembly-competent building blocks, the morphogenetic interactions that organize building blocks into procapsids, and the revised set of interactions that stabilize the mature capsid. In this context, we have addressed the question of how incorporation of VP26 into the capsid is regulated.

Expression, purification, and properties of VP26. Although the main aims of expressing a protein as a fusion are usually to increase its solubility and simplify purification, we used this strategy only to stabilize the expressed protein, albeit in an aggregated form. The simple purification and folding scheme that we have developed should be suitable for handling other insoluble GST fusion proteins.

Isolated VP26 has a high isoelectric point (11.2) and low

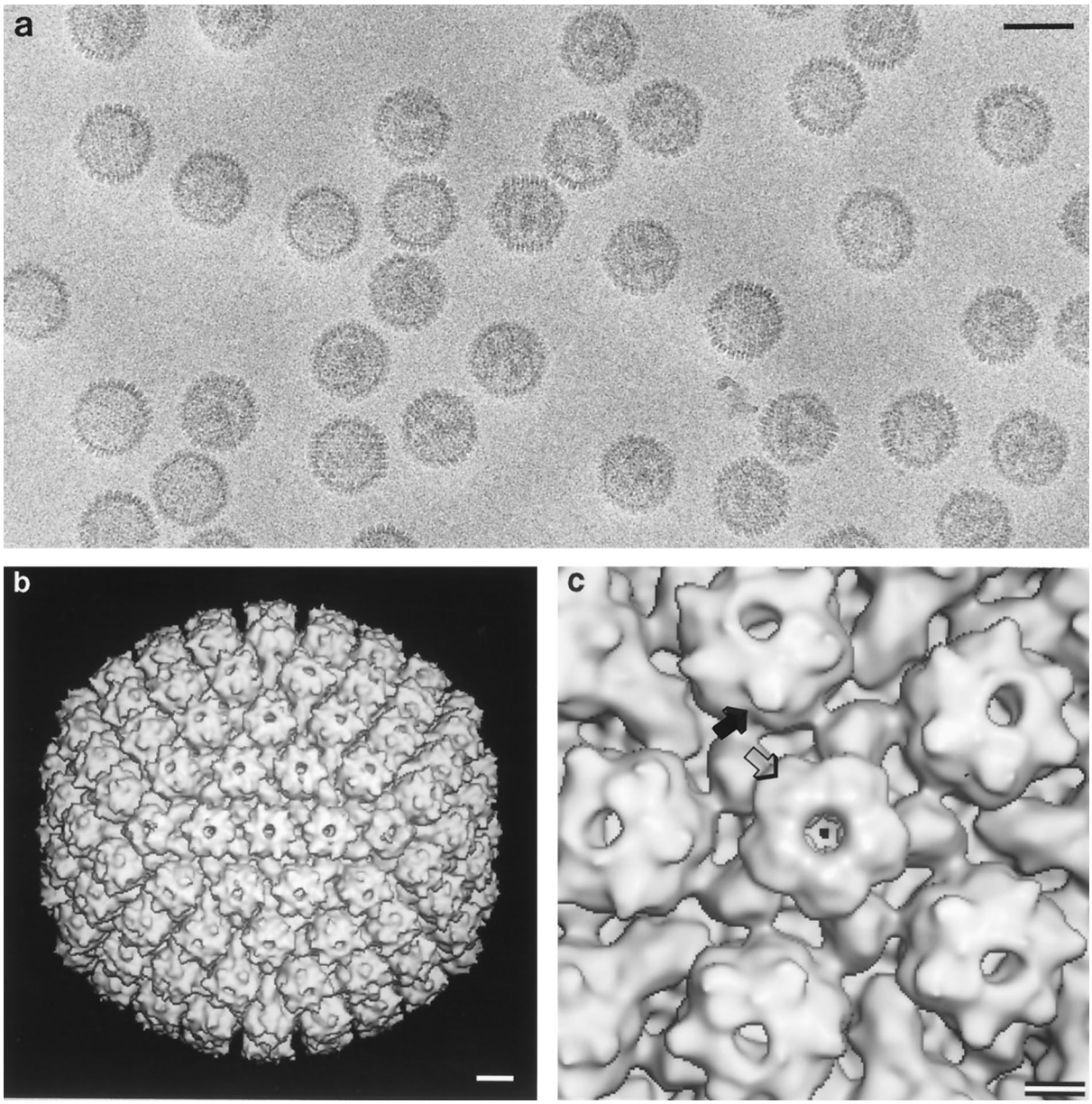

FIG. 5. (a) Cryo-electron micrograph of purified (All − UL35) HSV-1 capsids after in vitro complementation with an eightfold molar excess of purified VP26. Bar = 100 nm. (b) Three-dimensional structure of these capsids at 2.4-nm resolution, as viewed along a twofold axis of symmetry. Bar = 10 nm. (c) Blowup of the capsid structure around a penton site. Each hexon has six prominent horns of density around its outer rim (solid arrow), corresponding to six monomers of VP26. These features are absent from pentons (hollow arrow). Bar = 5 nm.

intrinsic solubility. Although we have not made a comprehensive investigation of solvent conditions, it was clear from the outset that both GST-VP26 and VP26 have low solubility in standard buffers, such as PBS. Aggregation can be partially prevented by increasing the ionic strength with NaCl. However, the key to maintaining solubility was the inclusion of CHAPS to at least 5 mM. The detergent did not affect either the conformation of VP26 or its ability to bind to capsids. However, even in the presence of detergent and high ionic strength, the solubility was limited to ~2 to 3 mg/ml. Thus solubilized, VP26 consists of a mixture of monomers and dimers. When studied in the absence of detergent, with aggregates removed by high-speed centrifugation immediately beforehand, VP26 behaved in a similar manner (data not shown).

VP26's mode of binding to capsids. VP26 extracted from purified wild-type capsids by heating binds to capsids that lack this protein (22). We have now found that bacterially expressed VP26 also binds faithfully to the hexons of acceptor capsids while the pentons remain unoccupied, even with a high molar excess of VP26. Its binding is unaffected by the three additional amino acids present at its N terminus; in fact, the entire GST-VP26 fusion protein appears to be capable of binding to capsids (preliminary observations [not shown]).

Previously, we have visualized VP26 subunits around the rims of VP5 hexons in two difference maps at ~30-Å resolution: one from pentonless Gdn-HCl-extracted capsids with and without VP26 (7), and the other between two kinds of baculovirus-derived capsids, All and (All − UL35) (38). In both

cases, we found it difficult to decide whether the six VP26 monomers per hexon actually make contact with each other, since this feature was acutely sensitive to the choice of threshold used for contouring. From their difference map at ~20 Å resolution between wild-type B capsids and baculovirus-derived (All − UL35) capsids, Zhou et al. (42) described the VP26 monomer as consisting of a large and a small domain, with six monomers forming a continuous ring. Since VP26 in solution consists of monomers and dimers, it follows that such contacts as exist between VP26 subunits on capsids are not extensive enough to promote hexamerization in the absence of the underlying template of a VP5 hexon. Alternatively, the conformation of VP26 may change upon binding to the capsid, to allow formation of intersubunit contacts.

Our sedimentation analysis indicates that purified VP26 observes a monomer-dimer equilibrium, with no evidence for hexamers or other oligomers higher than the dimer. We conclude, therefore, that its disinclination to bind to pentons reflects the absence of binding sites on pentons. It follows that the surface residues of VP5 which form the VP26 binding site on hexons must be conformed differently on pentons, so as to abrogate binding.

VP26 binding in intracellular capsid assembly. We note that incorporation of VP26 may occur differently in vivo. VP26 has no known nuclear import signal, and Rixon and coworkers have reported that an association with VP5 is necessary for VP26 to enter the nucleus (29). What happens next is unclear, but we may consider several possibilities. The transported complexes may enter the nucleus intact, or they may dissociate upon traversing the nuclear envelope. In the nucleus, VP5 may be present both with and without VP26, with the latter molecules being selectively incorporated into nascent procapsids at vertex sites. Alternatively, all VP5 molecules may be charged with VP26, with VP26 molecules being released when their VP5 partners adapt to the penton conformation. At present, we are unable to distinguish between these (and other) possibilities. However, as noted above, VP26 is not very soluble, implying that in vivo it is likely to be engaged, for the most part, in complexes of one kind or another.

Functional implications: a mechanism for diversifying the binding sites presented on the capsid surface. Although VP26 is not required for capsid assembly, other observations imply that it is of some utility to the virus. These include its high copy number (900) and evolutionary persistence. With the sole exception of the distant relative, channel catfish virus (6, 13), a VP26 counterpart has been detected in every herpesvirus studied to date. Moreover, a recent preliminary report has been made of a VP26-null mutant that is capable of replication in cultured cells but is 30-fold less efficient than the wild-type allele in propagating in trigeminal ganglia (14). Other conserved properties include genetic setting—close to the major capsid protein gene and in the opposite polarity, basic charge, and generally low MW. However, compared with other herpesvirus capsid proteins (6), the size of VP26-like proteins is not closely conserved, ranging from 75 amino acids for human cytomegalovirus (16) to 176 for Epstein-Barr virus (19). VP26 of HSV-1 has 116 amino acids. Nor is there much sequence similarity between VP26 and its counterparts in other herpesviruses, although homologies are evident between the members of this family expressed by several gammaherpesviruses (19).

As previously noted (6), its exposed site suggests that VP26 is well placed to couple the capsid to functional partners, such as the tegument, in the final phase of virion assembly. However, the capsid must also engage in different interactions at other stages of the replicative cycle, for instance, with molecular motors in cytoplasmic transport subsequent to cell entry (25, 32) and with nuclear pores, when discharging the viral genome into the nucleus of an infected cell (4). In this context, it is plausible that the device of leaving some capsomers (pentons) bare and decorating others (hexons) with an adapter protein, VP26, would confer the advantage of expanding the range of functional binding sites on the capsid surface.

ACKNOWLEDGMENTS

We thank Ira Palmer and Josh Kaufman for expert help in protein expression and purification, Pat Spinella for N-terminal sequencing, and T. Baker and J. Conway for software.

REFERENCES

1. **Baker, T. S., and R. H. Cheng.** 1996. A model-based approach for determining orientations of biological macromolecules imaged by cryoelectron microscopy. J. Struct. Biol. **116:**120–130.
2. **Baker, T. S., J. Drak, and M. Bina.** 1988. Reconstruction of the three-dimensional structure of simian virus 40 and visualization of the chromatin core. Proc. Natl. Acad. Sci. USA **85:**422–426.
3. **Baker, T. S., J. Drak, and M. Bina.** 1989. The capsid of small papova viruses contains 72 pentameric capsomeres: direct evidence from cryo-electron-microscopy of simian virus 40. Biophys. J. **55:**243–253.
4. **Batterson, W., D. Furlong, and B. Roizman.** 1983. Molecular genetics of herpes simplex virus. VIII. Further characterization of a temperature-sensitive mutant defective in release of viral DNA and in other stages of the viral replicative cycle. J. Virol. **45:**397–407.
5. **Booy, F. P., W. W. Newcomb, B. L. Trus, J. C. Brown, T. S. Baker, and A. C. Steven.** 1991. Liquid-crystalline, phage-like, packing of encapsidated DNA in herpes simplex virus. Cell **64:**1007–1015.
6. **Booy, F. P., B. L. Trus, A. J. Davison, and A. C. Steven.** 1996. The capsid architecture of channel catfish virus, an evolutionarily distant herpesvirus, is largely conserved in the absence of discernible sequence homology with herpes simplex virus. Virology **215:**134–141.
7. **Booy, F. P., B. L. Trus, W. W. Newcomb, J. C. Brown, J. F. Conway, and A. C. Steven.** 1994. Finding a needle in a haystack: detection of a small protein (the 12 kDa VP26) in a large complex (the 200 MDa capsid of herpes simplex virus). Proc. Natl. Acad. Sci. USA **91:**5652–5656.
8. **Cohen, G. H., M. Ponce de Leon, H. Diggelmann, W. C. Lawrence, S. K. Vernon, and R. J. Eisenberg.** 1980. Structural analysis of the capsid polypeptides of herpes simplex virus types 1 and 2. J. Virol. **34:**521–531.
9. **Cohn, E. J., and J. T. Edsall.** 1943. Proteins, amino acids and peptides. Van Nostrand-Reinhold, Princeton, N.J.
10. **Conway, J. F., B. L. Trus, F. P. Booy, W. W. Newcomb, J. C. Brown, and A. C. Steven.** 1993. The effects of radiation damage on the structure of frozen hydrated HSV-1 capsids. J. Struct. Biol. **111:**222–233.
11. **Conway, J. F., B. L. Trus, F. P. Booy, W. W. Newcomb, J. C. Brown, and A. C. Steven.** 1996. Visualization of three-dimensional density maps reconstructed from cryoelectron micrographs of viral capsids. J. Struct. Biol. **116:**200–208.
12. **Crowther, R. A.** 1971. Procedures for three-dimensional reconstruction of spherical viruses by Fourier synthesis from electron micrographs. Philos. Trans. R. Soc. Lond. Ser. B **261:**221–230.
13. **Davison, M. D., F. J. Rixon, and A. J. Davison.** 1992. Identification of genes encoding two capsid proteins (VP24 and VP26) of herpes simplex virus type 1. J. Gen. Virol. **73:**2709–2713.
14. **Desai, P., N. A. DeLuca, and S. Person.** The HSV-1 VP26 polypeptide is not essential for growth in cell culture but is important for virus pathogenesis. Submitted for publication.
15. **Fuller, S. D.** 1987. The T=4 envelope of Sindbis virus is organized by interactions with a complementary T=3 capsid. Cell **48:**923–934.
16. **Gibson, W., K. S. Clopper, W. J. Britt, and M. K. Baxter.** 1996. Human cytomegalovirus (HCMV) smallest capsid protein identified as product of short open reading frame located between HCMV UL48 and UL49. J. Virol. **70:**5680–5683.
17. **Heilman, C. J., Jr., M. Zweig, J. R. Stephenson, and B. Hampar.** 1979. Isolation of a nucleocapsid polypeptide of herpes simplex virus types 1 and 2 possessing immunologically type-specific and cross-reactive determinants. J. Virol. **29:**34–42.
18. **Laue, T. M., B. D. Shah, T. M. Ridgeway, and S. L. Pelletier.** 1992. Computer-aided interpretation of analytical sedimentation data for proteins, p. 90–125. *In* S. E. Harding, A. J. Rowe, and J. C. Horton (ed.), Analytical centrifugation in biochemistry and polymer science. Royal Society for Chemistry, Cambridge, England.
19. **Lin, S.-F., R. Sun, L. Heston, L. Gradoville, D. Shedd, K. Haglund, M. Rigsby, and G. Miller.** 1997. Identification, expression, and immunogenicity of Kaposi's sarcoma-associated herpes virus-encoded small viral capsid antigen. J. Virol. **71:**3069–3076.
20. **McNabb, D. S., and R. J. Courtney.** 1992. Posttranslational modification and subcellular localization of the p12 capsid protein on herpes simplex virus type 1. J. Virol. **66:**4839–4847.

21. **McNabb, D. S., and R. J. Courtney.** 1994. Identification and characterization of the herpes simplex virus type 1 virion protein encoded by the UL35 open reading frame. J. Virol. **66:**2653–2663.
22. **Newcomb, W. W., and J. C. Brown.** 1991. Structure of the herpes simplex virus capsid: effects of extraction with guanidine-HCl and partial reconstitution of extracted capsids. J. Virol. **65:**613–620.
23. **Newcomb, W. W., F. L. Homa, F. P. Booy, D. R. Thomsen, B. L. Trus, A. C. Steven, J. V. Spencer, and J. C. Brown.** 1996. Assembly of the herpes simplex virus capsid: characterization of intermediates observed during cell-free capsid formation. J. Mol. Biol. **263:**432–446.
24. **Newcomb, W. W., B. L. Trus, F. P. Booy, A. C. Steven, J. S. Wall, and J. C. Brown.** 1993. Structure of the herpes simplex virus capsid: molecular composition of the pentons and triplexes. J. Mol. Biol. **232:**499–511.
25. **Penfold, M. E., P. Armati, and A. L. Cunningham.** 1994. Axonal transport of herpes simplex virions to epidermal cells: evidence for a specialized mode of virus transport and assembly. Proc. Natl. Acad. Sci. USA **91:**6529–6533.
26. **Pepinsky, R. B.** 1990. Selective precipitation of proteins from guanidine hydrochloride-containing solutions with ethanol. Anal. Biochem. **195:**177–181.
27. **Provencher, S. W., and J. Gloeckner.** 1981. Estimation of globular protein secondary structure from circular dichroism. Biochemistry **20:**33–37.
28. **Rixon, F. J.** 1993. Structure and assembly of herpesviruses. Semin. Virol. **4:**135–144.
29. **Rixon, F. J., C. Addison, A. McGregor, S. J. Macnab, P. Nicholson, V. G. Preston, and J. D. Tatman.** 1996. Multiple interactions control the intracellular localization of the herpes simplex virus type 1 capsid proteins. J. Gen. Virol. **77:**2251–2260.
30. **Rost, B., and C. Sander.** 1994. Combining evolutionary information and neural networks to predict protein secondary structure. Proteins **19:**55–72.
31. **Scharf, S. J., G. T. Horn, and H. A. Erlich.** 1986. Direct cloning and sequence analysis of enzymically amplified genomic sequences. Science **233:**1076–1078.
32. **Sodeik, B., M. W. Ebersold, and A. Helenius.** 1997. Microtubule-mediated transport of incoming herpes simplex virus 1 capsids to the nucleus. J. Cell Biol. **136:**1007–1021.
33. **Steven, A. C., C. R. Roberts, J. Hay, M. E. Bisher, T. Pun, and B. L. Trus.** 1986. Hexavalent capsomers of herpes simplex virus type 2: symmetry, shape, dimensions, and oligomeric status. J. Virol. **57:**578–584.
34. **Steven, A. C., and P. G. Spear.** 1997. Herpesvirus capsid assembly and envelopment, p. 312–351. *In* W. Chiu, R. M. Burnett, and R. L. Garcea (ed.), Structural biology of viruses. Oxford University Press, New York, N.Y.
35. **Tatman, J. D., V. G. Preston, P. Nicholson, R. M. Elliott, and F. J. Rixon.** 1994. Assembly of herpes simplex virus type 1 capsids using a panel of recombinant baculoviruses. J. Gen. Virol. **75:**1101–1113.
36. **Thomsen, D. R., L. L. Roof, and F. L. Homa.** 1994. Assembly of herpes simplex virus (HSV) intermediate capsids in insect cells infected with recombinant baculoviruses expressing HSV capsid proteins. J. Virol. **68:**2442–2457.
37. **Trus, B. L., F. P. Booy, W. W. Newcomb, J. C. Brown, F. L. Homa, D. R. Thomsen, and A. C. Steven.** 1996. The herpes simplex virus procapsid: structure, conformational changes upon maturation, and roles of the triplex proteins VP19c and VP23 in assembly. J. Mol. Biol. **263:**447–462.
38. **Trus, B. L., F. L. Homa, F. P. Booy, W. W. Newcomb, D. R. Thomsen, N. Cheng, J. C. Brown, and A. C. Steven.** 1995. Herpes simplex virus capsids assembled in insect cells infected with recombinant baculoviruses: structural authenticity and localization of VP26. J. Virol. **69:**7362–7366.
39. **Trus, B. L., W. W. Newcomb, F. P. Booy, J. C. Brown, and A. C. Steven.** 1992. Distinct monoclonal antibodies separately label the hexons or the pentons of herpes simplex virus capsid. Proc. Natl. Acad. Sci. USA **89:**11508–11512.
40. **Venyaminov, S. Y., I. A. Baikalov, Z. M. Shen, C.-S. C. Wu, and J. T. Yang.** 1993. Circular dichroism analysis of denatured proteins: inclusion of denatured proteins in the reference set. Anal. Biochem. **214:**17–24.
41. **Wetlaufer, D. B.** 1962. Ultraviolet spectra of proteins and amino acids. Adv. Protein Chem. **17:**303–390.
42. **Zhou, Z. H., J. He, J. Jakana, J. D. Tatman, F. J. Rixon, and W. Chiu.** 1995. Assembly of VP26 in herpes simplex virus-1 inferred from structures of wild-type and recombinant capsids. Nat. Struct. Biol. **2:**1026–1030.
43. **Zhou, Z. H., B. V. V. Prasad, J. Jakana, F. J. Rixon, and W. Chiu.** 1994. Protein subunit structures in the herpes simplex virus capsid determined from 400-kV spot-scan electron cryomicroscopy. J. Mol. Biol. **242:**456–469.